

ϵ Subunit of *Bacillus subtilis* F_1 -ATPase Relieves MgADP Inhibition

Junya Mizumoto¹, Yuka Kikuchi¹, Yo-Hei Nakanishi¹, Naoto Mouri¹, Anrong Cai¹, Tokushiro Ohta¹, Takamitsu Haruyama^{1*}, Yasuyuki Kato-Yamada^{1,2}

¹ Department of Life Science, Rikkyo University, Tokyo, Japan, ² Research Center for Life Science, Rikkyo University, Tokyo, Japan

Abstract

MgADP inhibition, which is considered as a part of the regulatory system of ATP synthase, is a well-known process common to all F_1 -ATPases, a soluble component of ATP synthase. The entrapment of inhibitory MgADP at catalytic sites terminates catalysis. Regulation by the ϵ subunit is a common mechanism among F_1 -ATPases from bacteria and plants. The relationship between these two forms of regulatory mechanisms is obscure because it is difficult to distinguish which is active at a particular moment. Here, using F_1 -ATPase from *Bacillus subtilis* (BF_1), which is strongly affected by MgADP inhibition, we can distinguish MgADP inhibition from regulation by the ϵ subunit. The ϵ subunit did not inhibit but activated BF_1 . We conclude that the ϵ subunit relieves BF_1 from MgADP inhibition.

Citation: Mizumoto J, Kikuchi Y, Nakanishi Y-H, Mouri N, Cai A, et al. (2013) ϵ Subunit of *Bacillus subtilis* F_1 -ATPase Relieves MgADP Inhibition. PLoS ONE 8(8): e73888. doi:10.1371/journal.pone.0073888

Editor: Oleg Y. Dmitriev, University of Saskatchewan, Canada

Received: March 27, 2013; **Accepted:** July 23, 2013; **Published:** August 13, 2013

Copyright: © 2013 Mizumoto et al. This is an open-access article distributed under the terms of the Creative Commons Attribution License, which permits unrestricted use, distribution, and reproduction in any medium, provided the original author and source are credited.

Funding: This work was supported in parts by Grants-in-Aid for Scientific Research for Young Scientists (B) (No. 23770157), the Strategic Research Foundation Grant-aided Project for Private Universities (No. S1201003) from the Ministry of Education, Culture, Sports, Science and Technology of Japan, and Rikkyo University Special Fund for Research from Rikkyo University (to Y. K.-Y.). The funders had no role in study design, data collection and analysis, decision to publish, or preparation of the manuscript.

Competing interests: The authors have declared that no competing interests exist.

* E-mail: katoyama@rikkyo.ac.jp

‡ Current address: Bio-AFM Frontier Research Center, College of Science and Engineering, Kanazawa University

Introduction

FoF₁-ATPase/synthase (FoF₁) catalyzes ATP synthesis from ADP and inorganic phosphate coupled with the flow of H⁺ driven by the electrochemical gradient of H⁺ across cellular membranes. FoF₁ consists of a water-soluble ATP-driven F₁ motor (F₁-ATPase) connected to a membrane-embedded H⁺-driven Fo motor to couple ATP synthesis/hydrolysis and H⁺ flow via a unique rotary mechanism [1–4]. F₁-ATPase comprises α_3 , β_3 , γ , δ and ϵ subunits and its hydrolysis of one ATP molecule drives a discrete 120° rotation of the $\gamma\epsilon$ subunits relative to the others [5,6]. In FoF₁, rotation of the rotor subunits of F₁ (γ and ϵ) is transferred to the c subunit-ring of Fo to couple ATP synthesis/hydrolysis and flow of H⁺.

The smallest subunit, ϵ , is an endogenous inhibitor of the ATPase activity of bacterial and chloroplast F₁-ATPases and is believed to contribute to the regulation ATP synthase [7–10]. The mechanism of inhibition by the ϵ subunit (ϵ inhibition) varies among species. For example, when F₁-ATPase is separated from Fo, the ϵ subunit works as a dissociative inhibitor in *Escherichia coli* (EF₁) and plant chloroplasts (CF₁). The ϵ subunit inhibits ATPase activity, and the enzyme is reactivated when it dissociates from F₁-ATPase, and the addition of excess ϵ subunits restores inhibition. In contrast, the

ϵ subunit of F₁-ATPase from thermophilic *Bacillus* PS3 (TF₁) does not dissociate from the TF₁ complex, and the addition of excess ϵ subunits does not significantly inhibit activity [10]. Rather, the ϵ subunit controls the activation state of the enzyme by changing its conformation. Because the dissociation of the ϵ subunit may not occur within the ATP synthase holo-complex, the ϵ subunit of EF₁ or CF₁ may also work as a regulator in intact ATP synthase. When in the extended conformation, the C-terminal domain of the ϵ subunit elongates into the cavity of the $\alpha_3\beta_3$ ring and inhibits ATPase activity [11–16]. Upon activation, the C-terminal α helices of the ϵ subunit are expelled from the $\alpha_3\beta_3$ ring and the ϵ subunit takes a folded-state conformation in which the C-terminal α helices are folded into a helix-turn-helix conformation, and ATPase activity is not inhibited [17]. We recently demonstrated that, in the case of TFoF₁, the coupling between ATPase activity and flow of H⁺ is altered when the ϵ subunit does not bind ATP [18].

F₁-ATPase is most commonly regulated by MgADP inhibition [19–21], which affects all known ATP synthases, and it is caused by the entrapment of MgADP at the catalytic site(s). The recovery from MgADP inhibition is accelerated when ATP binds to non-catalytic sites [22–26]. MgADP inhibition can be observed as pauses of the rotation of the γ subunit [27]. The

pause angle of the γ subunit during MgADP inhibition is the same as that of the catalytic dwell (80° from the ATP-binding dwell), which is also the same as that during ε inhibition [28–30]. From this and other results, some investigators have proposed that ε inhibition is caused by the stabilization of MgADP inhibition [28,29,31]. Conversely, ε inhibition is prominent even in the presence of the detergent, lauryl dimethyl amine oxide (LDAO) (see supplemental figures of ref[14].), which is known to reduce MgADP inhibition [32]. Further, MgADP inhibition occurs even in the absence of the ε subunit. We demonstrated that the ε subunit greatly reduces the affinity of catalytic sites for MgATP and MgADP [10,33], which counteracts MgADP inhibition rather than stabilizing it. We have shown that the ε subunit relieved MgADP inhibition of a mutant TF₁ unable to bind nucleotides to non-catalytic sites although at low levels [30]. Sekiya et al. reported that the ε subunit does not significantly influence MgADP inhibition of *E. coli* F₁-ATPase [34]. Konno et al. proposed the existence of different origins of MgADP inhibition and ε inhibition in cyanobacterial F₁-ATPase [35]. This discrepancy may be explained by concurrent and indistinguishable MgADP inhibition and ε inhibition.

Although the FoF₁-ATP synthase from *Bacillus subtilis* has been studied for decades [36–38], to the best of our knowledge, no detailed kinetic analysis of the purified enzyme has been reported, particularly regarding ε inhibition or MgADP inhibition. To address this question, in the present study, we purified F₁-ATPase from *B. subtilis* (BF₁) and carried out detailed analyses of the relationship between MgADP inhibition and the function of the ε subunit. Because the activity of BF₁ is strongly affected by MgADP inhibition, we were able to examine the effect of the ε subunit on MgADP inhibition in detail. The results clearly indicate that regulation by the ε subunit is not only distinct from MgADP inhibition but their effects counteract each other.

Materials and Methods

Construction of a Plasmid to Express the α₃β₃γ Complex of BF₁

KOD-Plus DNA DNA polymerase (Toyobo) was used for PCR reactions. The region containing the genes encoding the α, γ, and β subunits of BF₁ was amplified by genomic PCR by using two primers as follows: 5'-CCGAATTCATATGAGCATCAAAGCTGAAGAGATTAGCACGC-3' contains *EcoRI* and *NdeI* sites. The initiation codon of the α subunit (GTG) was replaced with ATG; 5'-GGCTCGAGCTGCAGTTAACTTCTACACCCATTTCTTTTGC TTTC-3' contains *PstI* and *XhoI* sites and the termination codon for the β subunit. *B. subtilis* genomic DNA was used as template. The PCR product was cloned into the *EcoRV* site of the pZero2.1 vector (Invitrogen) to produce pZero-BF1. The initiation codon of the γ subunit was converted from TTG to ATG and the SD sequence of the γ subunit was converted from AAGG to AAGGAGG, as reported for the expression system of TF₁ [39] using overlap-extension PCR [40,41] with the four primers as follows: The mutagenic primers, 5'-AGAGAAAAGGAGGTGAAATCCATGGCCTCATTACG-3' and

5'-AATGAGGCCATGGATTTACCTCCTTTTCTCTTC-3' contain an *NcoI* site in addition to the modifications described above; flanking primers were 5'-GCTGTCCTTGCTTCTTCGCCGTCGCCG-3' and 5'-TCTTGTTGATGGCTGCTTGGCGAG-3'. The resulting 1.6-kbp fragment, containing segments of the genes encoding the γ and α subunits, was cloned into the *EcoRV* site of pZero2.1. A 1-kbp *BglII* fragment containing the initiation codon for the γ subunit was transferred to the cognate site of pZero-BF1 in the correct orientation to generate pZero-BF1ATG. The full-length genes encoding the α, γ, and β subunits were excised from pZero-BF1ATG with *NdeI* and *XhoI* and cloned into the respective sites of the pET16b expression vector (Novagen), generating pET16b-BF1 in which a His₁₀-tag was introduced at the N-terminus of the α subunit. However, we were unable to express or purify the α₃β₃γ complex of BF₁ from this construct as most of the α subunits were expressed as monomers. To introduce the His₆-tag at the N-terminus of the β subunit, overlap-extension PCR was carried out using the four primers as follows: The mutagenic primers containing the His₆-tag were 5'-

CGATGCATCATCATCATCACATGAAGAAAGGACGCGT TAGCCAGG-3' and 5'-CTTCATGTGATGATGATGATGATGATGCATCGCTATCCCTCT GACAAAATC-3'. The flanking primers were 5'-CAGTTCGGTTTTACGGAGTGCTTATC-3' and 5'-GCGCCGGGTCAGTGTAGTCATCG-3'. The resulting 1.6-kbp fragment, which contained the region around the initiation codon for the β subunit, was cloned into the *EcoRV* site of pZero2.1 to generate pZero2.1-βhis. To remove the His₁₀-tag at the N-terminus of the α subunit, the *NdeI/XhoI*-digested fragment of pET16b-BF1, which contains the genes for the α, γ, and β subunits, was transferred to the respective sites of pET21a (Novagen) to produce pET21-BF1nohis. Then, to introduce the His₆-tag into the β subunit in pET21-BF1nohis, pZero2.1-βhis was digested with *BseRI/BssSI*. A 0.8-kbp fragment, which contained the N-terminus of the β subunit was isolated and ligated to a 7.2-kbp fragment of pET21-BF1nohis-digested with *BseRI/DrallI*, and a 1.3-kbp fragment, which contained most of the β subunit gene of pET21-BF1nohis, which was digested with *BssSI/DrallI*, to obtain pET21-BF1. The final product, pET21-BF1, contained the following modifications of the original genes as follows: the His₆-tag was introduced at the N-terminus of the β subunit, the initiation codon of the γ subunit was replaced with ATG, the SD sequence of the γ subunit was modified, an *NdeI* site was introduced at the 5'-terminus of the α subunit gene, and an *NcoI* site was introduced at the 5'-terminus of the γ subunit gene.

Construction of plasmids to express mutant proteins

The plasmid expressing the mutant (γ^{S3C}) α₃β₃γ complex of BF₁ was constructed as follows. The sequence of the genes encoding the entire γ subunit and part of the β subunit were amplified by PCR from pET21-BF1 with the primers as follows. The mutagenic primer was 5'-AAATCCATGGCCTGTTTACGCGATATTAAG-3', which contains a γSer3 to Cys substitution, and the other primer was

5'-ATGTAAGGAGCAAGCAAATCAACAAC-3'. The resulting 1.3-kbp fragment was introduced into the *EcoRV* site of pZero2.1 to produce pZero- γ S3C. Then, pZero- γ S3C was digested with *NcoI/SalI*, and a 1-kbp fragment containing the γ ^{S3C} region was recovered and ligated to a 7.4-kbp fragment of pET21-BF1 digested with *MunI/SalI*, and a 0.9-kbp fragment of *MunI/NcoI*-digested pET21-BF1, which contained a segment of the gene encoding the α subunit, was ligated to obtain pET21-BF1 (γ S3C). The plasmid expressing a mutant BF₁ ϵ subunit (133C, where a Cys was introduced at the C-terminus) was constructed using the following primers for PCR as follows: 5'-GCCGGCGAAGCTTAACATTTCCCTGCTAC-3', which contains 133C at the C-terminus of the BF₁ ϵ subunit and a *HindIII* site, and 5'-GAAATTAATACGACTCACTATAGG-3', which corresponds to the upstream sequence of the gene encoding the BF₁ ϵ subunit (T7 promoter). The expression plasmid for WT BF₁ ϵ [42] was used as the template. The resulting DNA fragment was cloned into the *EcoRV* site of pZero2.1; the resulting plasmid was digested with *NdeI/HindIII*, and the DNA fragment was transferred to the respective cognate sites of the pET21b expression vector to produce pET21-BF1 ϵ (133C).

Protein purification

WT or mutant (γ ^{S3C}) $\alpha_3\beta_3\gamma$ complexes of BF₁ were prepared as follows: *E. coli* BL21(DE3) was transformed with pET21-BF₁ and grown in 1-L LB medium containing 100 mg/L ampicillin and 10 μ M IPTG at 25° C for 24–36 h with vigorous shaking at 250 rpm in a 3-L baffled flask. Typically, approximately 6 g wet cells was produced. Cells were suspended in buffer A (20 mM Tris-H₂SO₄ (pH 7.5), 300 mM K₂SO₄, and 30 mM imidazole) to 0.1–0.2 g cells/ml and disrupted using a French Press. The rest of the procedures was carried out at 25° C. Cell debris was removed by centrifugation at 2,000 \times *g* for 15 min at 25° C. The supernatant was diluted with the same volume of buffer A and applied to a 5 ml HisTrapFF crude column (GE Healthcare Life Sciences) equilibrated with buffer A at a flow rate at 2 ml/min. The column was washed with buffer A until the absorbance at 280 nm plateaued. The adsorbed proteins were eluted with buffer B (buffer A containing 500 mM imidazole) and collected. Fractions were purified using a gel-filtration column (Superdex 200 10/300 GL; GE Healthcare Life Sciences) equilibrated with buffer C (50 mM Tris-H₂SO₄ (pH 7.5) and 50 mM K₂SO₄), eluted at 0.5 ml/min, monitored at 280 nm. The peak fractions containing $\alpha_3\beta_3\gamma$ complex were pooled, adjusted to 65% saturated ammonium sulfate, and stored in suspension at 4° C. Approximately 15 mg of $\alpha_3\beta_3\gamma$ complex was obtained from a 1-L culture. Purified $\alpha_3\beta_3\gamma$ complex did not contain bound nucleotides (<0.06 mol/mol) as measured by HPLC [43]. The $\alpha_3\beta_3\gamma$ complex was collected by centrifugation and dissolved in 50 mM Tris-H₂SO₄ (pH 7.5) and 50 mM K₂SO₄.

The WT ϵ subunit of BF₁ was purified as described previously [42], and the mutant ϵ ^{133C} subunit was purified as follows. Approximately 3 g of BL21(DE3)/pET21-BF1- ϵ (133C) cultivated as described previously [42], was suspended to ~0.2 g of wet cells/ml in buffer D (50 mM Tris-HCl (pH 8.0), 1 mM EDTA, 1 mM DTT, and protease inhibitor cocktail (Roche Diagnostics)) and then disrupted twice using a French Press.

The cell lysate was centrifuged at 3,000 \times *g* for 10 min at 4° C to remove cell debris, and the supernatant was centrifuged at 180,000 \times *g* for 1 h at 4° C. The rest of the procedures was carried out at 25° C. The supernatant was applied to a DEAE Toyopearl column (40 ml, Tosoh) equilibrated with buffer D. The flow-through fractions containing the ϵ ^{133C} subunit were collected and solid ammonium sulfate was added to 65% saturation. The precipitate was stored at 4° C. The protein was collected by centrifugation at 6,000 \times *g* for 15 min at 4° C and dissolved in 30 mL of buffer D containing 10% saturated ammonium sulfate and applied to a butyl Toyopearl column (20 mL; Tosoh) equilibrated and washed with the same buffer. The ϵ ^{133C} subunit was eluted with buffer D at a flow rate at ~3 ml/min and fractions containing the ϵ ^{133C} subunit were pooled, and solid ammonium sulfate was added to 65% saturation and stored at 4° C. Approximately 40 mg of ϵ ^{133C} was obtained from a 1-L culture. The ϵ ^{133C} subunit was collected for analysis by centrifugation and dissolved in 50 mM Tris-H₂SO₄ (pH 7.5) and 50 mM K₂SO₄.

ATPase assay

ATPase activity was measured spectrophotometrically with an ATP-regenerating system coupled to NADH oxidation at 25° C [44]. The assay mixture (1.5 ml) consisted of 50 mM Tris-H₂SO₄ (pH 7.5), 50 mM K₂SO₄, 2 mM phosphoenolpyruvate, 2 mM MgSO₄, 0.2 mM NADH, 50 μ g/ml pyruvate kinase, 50 μ g/ml lactate dehydrogenase, and the indicated concentration of ATP-Mg (equimolar mixture of ATP and MgSO₄) was transferred to a glass cuvette. Absorbance at 340 nm was measured using a V-550 spectrophotometer (JASCO) at 0.5 or 1-s intervals. The $\alpha_3\beta_3\gamma$ complex with or without ϵ subunit was added 2 min after starting the measurements. The mixture was stirred with a magnetic stirrer for 5 s before and after the addition of $\alpha_3\beta_3\gamma$ complex. The rate of ATP hydrolysis was determined from the rate of NADH oxidation. The final concentration of $\alpha_3\beta_3\gamma$ complex was 30 nM when measuring ATPase activity in the absence of lauryldimethylamine oxide (LDAO). Typically, 15 μ l of 3 μ M $\alpha_3\beta_3\gamma$ complex solution was added to 1.5 ml of the assay mixture. When ATPase activity was measured in the presence of LDAO, the final concentration of $\alpha_3\beta_3\gamma$ complex was reduced to 3 nM. In that case, 0.1 mg/ml bovine serum albumin (BSA) was included in stock $\alpha_3\beta_3\gamma$ complex solution (450 nM) to avoid the adsorption of $\alpha_3\beta_3\gamma$ complex on the plastic tube. Ten microliters of $\alpha_3\beta_3\gamma$ complex solution (450 nM) was added to 1.5 ml of the assay mixture without LDAO. Then, LDAO (final concentration 0.1%) was added and the solution was stirred continuously. When the ATPase activity of $\alpha_3\beta_3\gamma\epsilon$ complexes was measured, the ϵ subunit was included in the $\alpha_3\beta_3\gamma$ complex stock solution at a 1:10 (3 μ M $\alpha_3\beta_3\gamma$ complex and 30 μ M ϵ in the absence of LDAO) to 1:100 (450 nM $\alpha_3\beta_3\gamma$ complex and 45 μ M ϵ in the presence of LDAO) molar ratio. Reaction rates were determined at 2–7 s (initial) and 12–13 min (steady-state) after adding BF₁. The reaction rate in the presence of LDAO was determined 100–150 s after the addition of LDAO.

Preincubation with MgADP

The effect of preincubation with MgADP was determined as follows: BF₁ (10 μ M $\alpha_3\beta_3\gamma$ complex \pm 100 μ M ϵ) in 50 mM Tris-H₂SO₄ (pH 7.5), 50 mM K₂SO₄, and 4 mM MgSO₄ was mixed with an equal volume of 2 \times MgADP (equimolar mixture of ADP and MgSO₄) and incubated for more than 10 min at 25° C (Mg²⁺ concentration was in 2 mM excess ADP). Nine microliters of the mixture was added to 1.5 ml of ATPase assay mixture containing 2 mM MgATP (30 nM $\alpha_3\beta_3\gamma$ complex \pm 300 nM ϵ). The initial rate (2–4 s after the addition of BF₁) was determined in this experiment.

Crosslinking γ and ϵ subunits

Crosslinking of the γ subunit to the extended conformation of the ϵ subunit in $\alpha_3\beta_3\gamma^{\text{S3C}}\epsilon^{\text{133C}}$ was performed as follows. Ammonium sulfate suspensions of $\alpha_3\beta_3\gamma^{\text{S3C}}$ complex and ϵ^{133C} were centrifuged individually at 20,000 \times g for 15 min at 4° C. Each precipitate was dissolved in 50 mM Tris-H₂SO₄ (pH 7.5) and 50 mM K₂SO₄, and 10 mM DTT was added and incubated for 10 min at 25° C. The $\alpha_3\beta_3\gamma^{\text{S3C}}$ and ϵ^{133C} were mixed at a 1:10 molar ratio and incubated for 15 min at 25° C. Excess ϵ^{133C} was removed by ultrafiltration with a centrifugal concentrator (Amicon Ultra, 100-kDa cutoff). The sample was concentrated to approximately 10-fold and ultrafiltration was repeated 3 times after the addition of the same buffer to the original volume. The sample (1 mg/ml) was incubated with or without 4 mM MgATP for 10 min at 25° C; the solution was divided into two tubes, and an equal volume of 100 μ M CuCl₂ or the buffer was added. After 1-h incubation at 25° C, 10 mM EDTA was added to terminate the reaction. After 10 min, 0.1% SDS and 15 mM *N*-ethyl maleimide were added. The samples were analyzed using non-reducing SDS-PAGE (12% acrylamide). Part of the sample without ATP and with CuCl₂ was saved after the addition of 10 mM EDTA for the ATPase assay. A combination of WT $\alpha_3\beta_3\gamma$ complex and ϵ^{133C} served as the control. During the ATPase assays, 50 mM DTT was added to reduce crosslinking between the γ and ϵ subunits at the time indicated in the figure.

Other methods

Protein concentrations were determined by the method of Bradford [45] using BSA as a standard. DNA sequences for all of the recombinant proteins were confirmed using an ABI 3130xl Genetic Analyzer (Applied Biosystems). Non-reducing PAGE was performed according the method of Laemmli [46]. Chemicals were of the highest grade available. Kinetic data analyses were performed using Spectra Manager (JASCO) and OriginPro 8.5 and 9.0 (OriginLab), and the kinetic parameters are expressed with standard errors.

Results

ATPase activity of BF₁ and the effect of ϵ subunit

Typical time courses of ATP hydrolysis by $\alpha_3\beta_3\gamma$ and $\alpha_3\beta_3\gamma\epsilon$ complexes of BF₁ are shown in Figure 1. At ATP concentrations \geq 20 μ M, very large initial inactivation was observed, irrespective of the presence of the ϵ subunit. At ATP

concentrations $>$ 50 μ M, the inactivation was rapid enough to achieve constant, steady-state ATPase activity within the measurement (13 min), and there were no significant differences between $\alpha_3\beta_3\gamma$ and $\alpha_3\beta_3\gamma\epsilon$ at ATP concentrations $>$ 200 μ M (Figure 1A, B). At lower ATP concentrations, the rate of inactivation slowed and did not reach the steady state (Figure 1C). Under these conditions, the ATPase activity of $\alpha_3\beta_3\gamma\epsilon$ (lower traces in Figure 1) was higher than that of $\alpha_3\beta_3\gamma$. Inactivation was diminished at lower ATP concentrations (Figure 1D). Reaction rates determined at 2–7 s and 12–13 min as a function of ATP concentration are shown in Figure 2. The steady-state ATPase activity of BF₁ exhibited a decrease between 10 and 100 μ M ATP possibly due in part to slow inactivation that did not reach the steady-state at low ATP concentrations. The value of k_{cat} (1.83 s⁻¹ for $\alpha_3\beta_3\gamma$ and 1.80 s⁻¹ for $\alpha_3\beta_3\gamma\epsilon$) for steady-state ATPase activity is very low compared with the F₁-ATPases from other sources, for example, TF₁ \sim 60 s⁻¹ and EF₁ \sim 75 s⁻¹ at 25° C [39,47]. The ATPase activity increased more than 100-fold by LDAO, which is known to relieve MgADP inhibition (Figure 2). Because the initial rate of ATP hydrolysis reached only about 80 s⁻¹ (Figure 2), and 200 mM Pi, which is known to reduce MgADP inhibition [48], activated BF₁ to only \sim 10-fold (data not shown), the effect of LDAO may not be entirely related to MgADP inhibition. Nevertheless, these findings indicate that the ATPase activity of $\alpha_3\beta_3\gamma$ and $\alpha_3\beta_3\gamma\epsilon$ complexes of BF₁ was highly suppressed by MgADP inhibition. Judging from the activation ratio by LDAO, the degree of MgADP inhibition is low at low ATP concentrations. This could account for the triphasic dependence on ATP concentration dependence of ATPase activity in the absence of LDAO in part. In the presence of LDAO, the concentration-dependence on ATP of ATPase activity followed simple sum of two Michaelis–Menten equations (Figure 2).

The ϵ subunit affected the ATPase activity of BF₁ only at low concentrations of ATP (Figures 1 and 2). Surprisingly, no inhibitory effect of the ϵ subunit was observed, and activation by the ϵ subunit occurred at ATP concentrations $<$ 50 μ M (Figure 1C, D, lower trace). The dissociation of ϵ subunit from $\alpha_3\beta_3\gamma\epsilon$ complex may not account for the equivalent activities of $\alpha_3\beta_3\gamma$ and $\alpha_3\beta_3\gamma\epsilon$ at high ATP concentrations, because the $\alpha_3\beta_3\gamma\epsilon$ complex could be isolated by gel-filtration HPLC (Superdex 200 10/300GL) even in the presence of ATP and/or LDAO (data not shown). Further, the addition of up to 30 μ M ϵ subunit to the ATPase assay mixture did not significantly affect steady-state ATPase activity at 2 mM ATP (data not shown). In the presence of LDAO, the ATPase activities of $\alpha_3\beta_3\gamma$ and $\alpha_3\beta_3\gamma\epsilon$ were essentially the same at all ATP concentrations, although the k_{cat} value of $\alpha_3\beta_3\gamma\epsilon$ (352 s⁻¹) was slightly higher than that of $\alpha_3\beta_3\gamma$ (268 s⁻¹) (Figure 2). The initial rates of ATP hydrolysis were also not significantly different (Figure 2). Therefore, the inhibition by the ϵ subunit of BF₁ might be very weak, if any.

Preincubation with MgADP

When $\alpha_3\beta_3\gamma$ was preincubated with MgADP, the initial ATPase activity was significantly inhibited (Figure 3, closed circles), as reported previously for other F₁-ATPases [26,48].

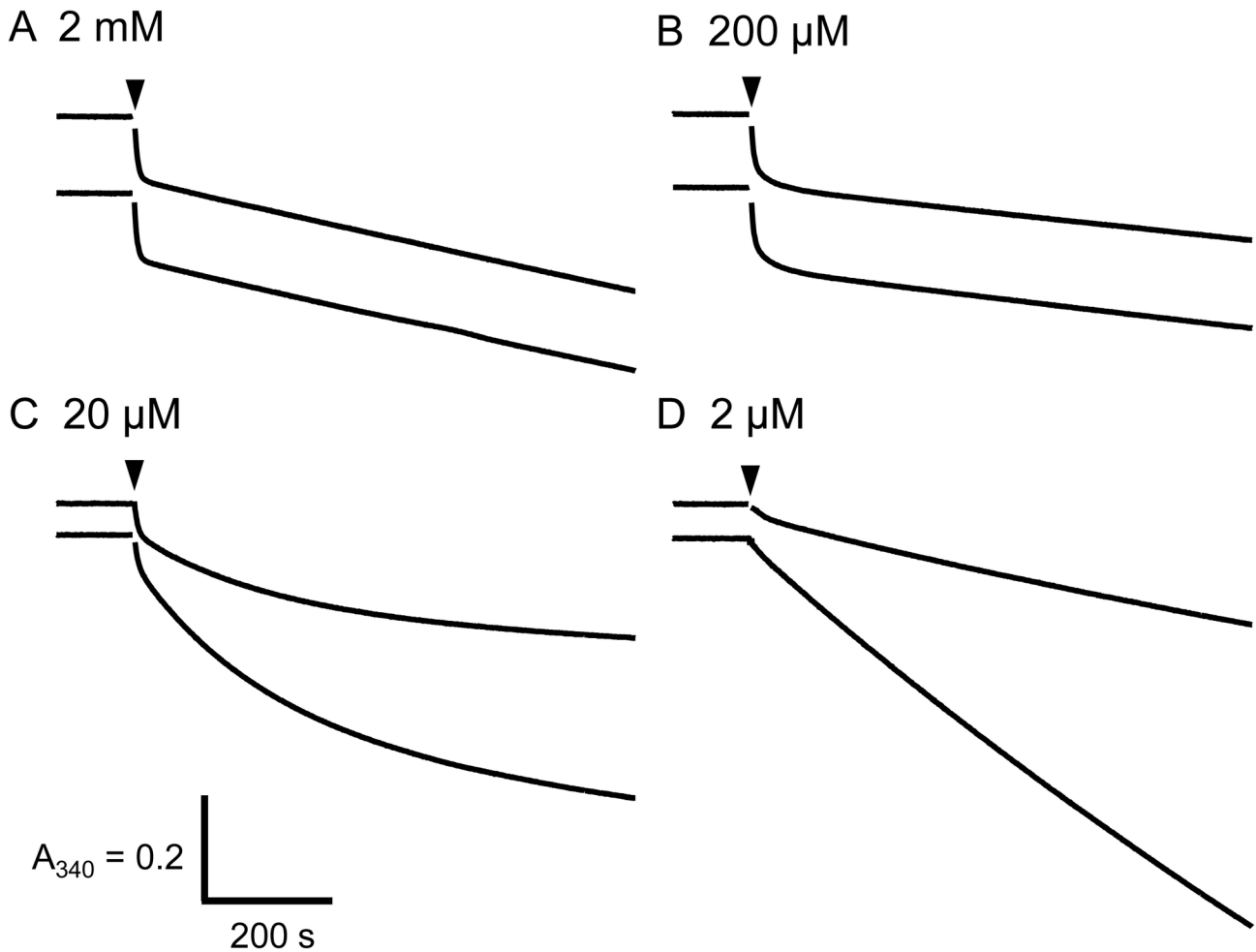


Figure 1. Time-course of ATP hydrolysis by BF₁ with or without the ϵ subunit. In each panel, the upper and lower traces represent $\alpha_3\beta_3\gamma$ and $\alpha_3\beta_3\gamma\epsilon$, respectively. The final concentration of $\alpha_3\beta_3\gamma$ or $\alpha_3\beta_3\gamma\epsilon$ complex of BF₁ was 30 nM. The ATP concentrations are indicated in the figure. The $\alpha_3\beta_3\gamma$ or $\alpha_3\beta_3\gamma\epsilon$ complex of BF₁ was added at the time indicated by the arrowheads. The vertical and horizontal bars denote 0.2 absorbance units and 200 s, respectively.

doi: 10.1371/journal.pone.0073888.g001

Incubation of 5 μ M $\alpha_3\beta_3\gamma$ with 1:1 and 1:2 MgADP resulted in about 50% and 70% inhibition, respectively. In the presence of the ϵ subunit (open circles), the ATPase activity of $\alpha_3\beta_3\gamma\epsilon$ was inhibited only marginally compared with that of $\alpha_3\beta_3\gamma$; incubation with 1:1 and 1:2 MgADP resulted in about 20% and 35% inhibition, respectively. Reduced inhibition by the preincubating $\alpha_3\beta_3\gamma\epsilon$ with MgADP might be due to the suppression of MgADP binding by the ϵ subunit in its extended conformation.

Catalytic properties of mutant BF₁ with its ϵ subunit fixed in the extended conformation

The activation by the ϵ subunit was investigated in more detail by examining a mutant $\alpha_3\beta_3\gamma\epsilon$ complex of BF₁, in which the N-terminus of the γ subunit and C-terminus of the ϵ subunit can be crosslinked via engineering in Cys residues to fix the ϵ subunit in the extended conformation. Thus, a mutant

equivalent to that of TF₁ [13] was prepared. The endogenous Cys residues in the α subunit did not react with the introduced Cys residues in the γ or ϵ subunits. To determine whether the apparent absence of ϵ inhibition in BF₁ resulted from the inability of the ϵ subunit to assume an extended conformation, the presence of γ - ϵ crosslink formation was determined in the presence or absence of ATP. The γ and ϵ bands disappeared and a band corresponding to the γ - ϵ crosslink product appeared only in the absence of ATP (Figures 4, and S2). The distance between the C α of the residues corresponding to the introduced Cys residues in a recently reported EF₁ structure is 12.9 Å [16]. Although this is a little bit long to form a disulfide bridge, the formation of a disulfide bridge within the mutant $\alpha_3\beta_3\gamma^{S3C}\epsilon^{133C}$ complex of BF₁ indicates that the crosslinked structure may reflect the physiological conformation within the range of thermal fluctuation. In the presence of ATP, a dimer of the ϵ subunit was formed, indicating that ϵ changed its

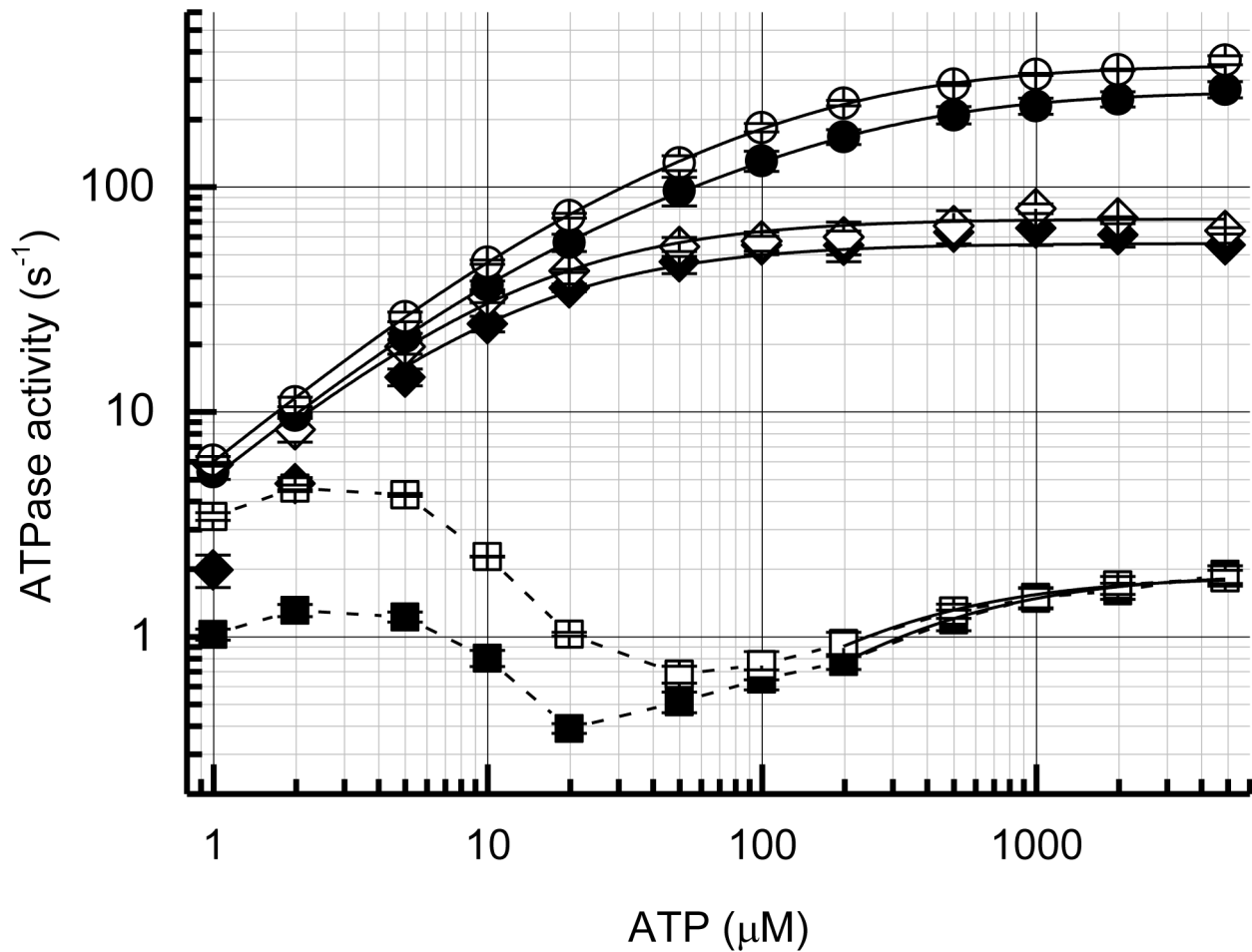


Figure 2. Dependence of BF₁ ATPase activity on ATP concentration. The ATPase activities of initial (*closed diamonds*; $\alpha_3\beta_3\gamma$, and *open diamonds*; $\alpha_3\beta_3\gamma\epsilon$), steady-state (*closed squares*; $\alpha_3\beta_3\gamma$, and *open squares*; $\alpha_3\beta_3\gamma\epsilon$) and in the presence of LDAO (*closed circles*; $\alpha_3\beta_3\gamma$, and *open circles*; ATPase activities of $\alpha_3\beta_3\gamma\epsilon$) at each ATP concentration was calculated from the velocities at 2–7 s, 12–13 min after the start of the reaction, and 100–150 s after the addition of LDAO, respectively. Error bars represent standard errors. The solid lines were fitted to a single (initial and steady-state) or sum of two (in the presence of LDAO) Michaelis–Menten equation(s). Only data from 200 μM and the above concentrations of ATP were used to fit the steady-state rates of $\alpha_3\beta_3\gamma$ and $\alpha_3\beta_3\gamma\epsilon$. Data from 1 μM (and 2 μM , in the case of $\alpha_3\beta_3\gamma$) were not used to fit the initial rate. The K_M and the associated k_{cat} values are $12.7 \pm 0.9 \mu\text{M}$, $56.2 \pm 0.9 \text{ s}^{-1}$ ($\alpha_3\beta_3\gamma$, initial); $13.8 \pm 0.9 \mu\text{M}$, $72.3 \pm 1.3 \text{ s}^{-1}$ ($\alpha_3\beta_3\gamma\epsilon$, initial); $296 \pm 25 \mu\text{M}$, $1.92 \pm 0.06 \text{ s}^{-1}$ ($\alpha_3\beta_3\gamma$, steady-state); $209 \pm 18 \mu\text{M}$, $1.87 \pm 0.04 \text{ s}^{-1}$ ($\alpha_3\beta_3\gamma\epsilon$, steady-state); $16.0 \pm 1.9 \mu\text{M}$, $68.8 \pm 10.9 \text{ s}^{-1}$ and $184 \pm 32 \mu\text{M}$, $199 \pm 10 \text{ s}^{-1}$ ($\alpha_3\beta_3\gamma$, +LDAO); and $18.7 \pm 3.4 \mu\text{M}$, $80.1 \pm 19.2 \text{ s}^{-1}$ and $138 \pm 18 \mu\text{M}$, $272 \pm 18 \text{ s}^{-1}$ ($\alpha_3\beta_3\gamma\epsilon$, +LDAO).

doi: 10.1371/journal.pone.0073888.g002

conformation from the extended to the intermediate or folded-state in which the C-terminal Cys was accessible on the surface of the molecule. We conclude from these results that the absence of ϵ inhibition was not caused by the absence of its extended conformation. However, because there were no significant differences in the initial activities of WT $\alpha_3\beta_3\gamma$ and $\alpha_3\beta_3\gamma\epsilon$ complexes, the extended conformation of the ϵ subunit may readily change upon addition of ATP.

We next determined the ATPase activity of the crosslinked mutant $\alpha_3\beta_3\gamma^{S33C\epsilon^{133C}}$. In the absence of LDAO, the activity of the mutant was significantly higher than that of WT, even at 2 mM ATP (Figure 5A). When crosslinking was reduced by the

addition of 50 mM DTT, the activity gradually decreased to the same level as WT. The addition of LDAO after this reduction resulted in activation to the WT level. When LDAO was added before reduction, activation of ATPase activity was undetectable (Figure 5B). The subsequent addition of DTT resulted in full activation.

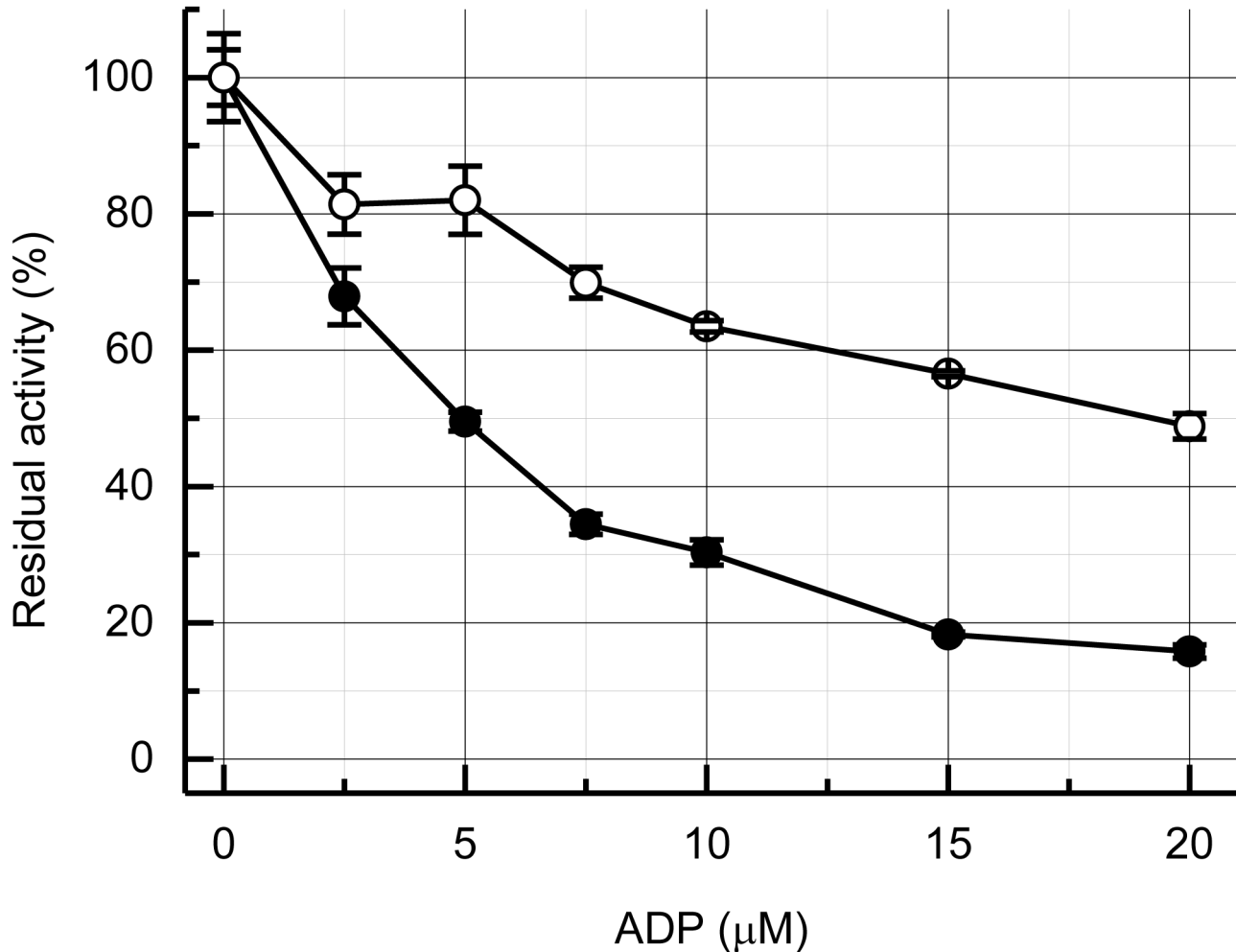


Figure 3. Effect of preincubation with MgADP. The $\alpha_3\beta_3\gamma$ or $\alpha_3\beta_3\gamma\epsilon$ (5 μM) was incubated with the indicated concentrations of MgADP for more than 10 min at 25° C. Residual ATPase activity was measured in the presence of 2 mM ATP. The initial rate (2–4 s after the start of the reaction) was measured, and the values relative to the control without incubation with MgADP ($82.9 \pm 5.4 \text{ s}^{-1}$ and $88.6 \pm 3.6 \text{ s}^{-1}$ for $\alpha_3\beta_3\gamma$ and $\alpha_3\beta_3\gamma\epsilon$, respectively) are plotted. Closed and open circles represent $\alpha_3\beta_3\gamma$ and $\alpha_3\beta_3\gamma\epsilon$, respectively. Error bars represent standard errors.

doi: 10.1371/journal.pone.0073888.g003

Discussion

ATPase activity of BF₁ is strongly suppressed by MgADP inhibition

BF₁ showed high initial ATPase activity, rapid inactivation, and very low steady-state ATPase activity. LDAO dramatically activated the steady-state ATPase activity of BF₁ (Figure 2). The initial ATPase activity was >20-fold higher than the steady-state ATPase activity, 200 mM Pi also activated steady-state ATPase activity by ~10-fold (data not shown), and preincubation with MgADP greatly suppressed the initial ATPase activity (Figure 3). These suggest that the inactivation might be due to strong MgADP inhibition, which could mean that the *B. subtilis* ATP synthase functions as an ATP synthase

that does not hydrolyze ATP, because MgADP inhibition does not inhibit ATP synthesis activity [49].

No inhibition by the ϵ subunit

The ϵ subunit did not significantly inhibit the ATPase activity of BF₁ but activated at low concentrations of ATP presumably due to the suppression of MgADP inhibition. Further, the ϵ subunit, fixed in the extended conformation, did not inhibit the mutant enzyme. The ϵ subunit only inhibited the activity of the extended-state fixed mutant $\alpha_3\beta_3\gamma^{\text{S3C-133C}}$ complex of BF₁ in the presence of LDAO (Figure 5B, S3C after addition of LDAO). In this case, DTT activated the enzyme, indicating that the activity before the addition of DTT was actually suppressed by the extended-state ϵ subunit. We conclude, therefore, that due to the strong MgADP inhibition, ϵ inhibition is not evident,

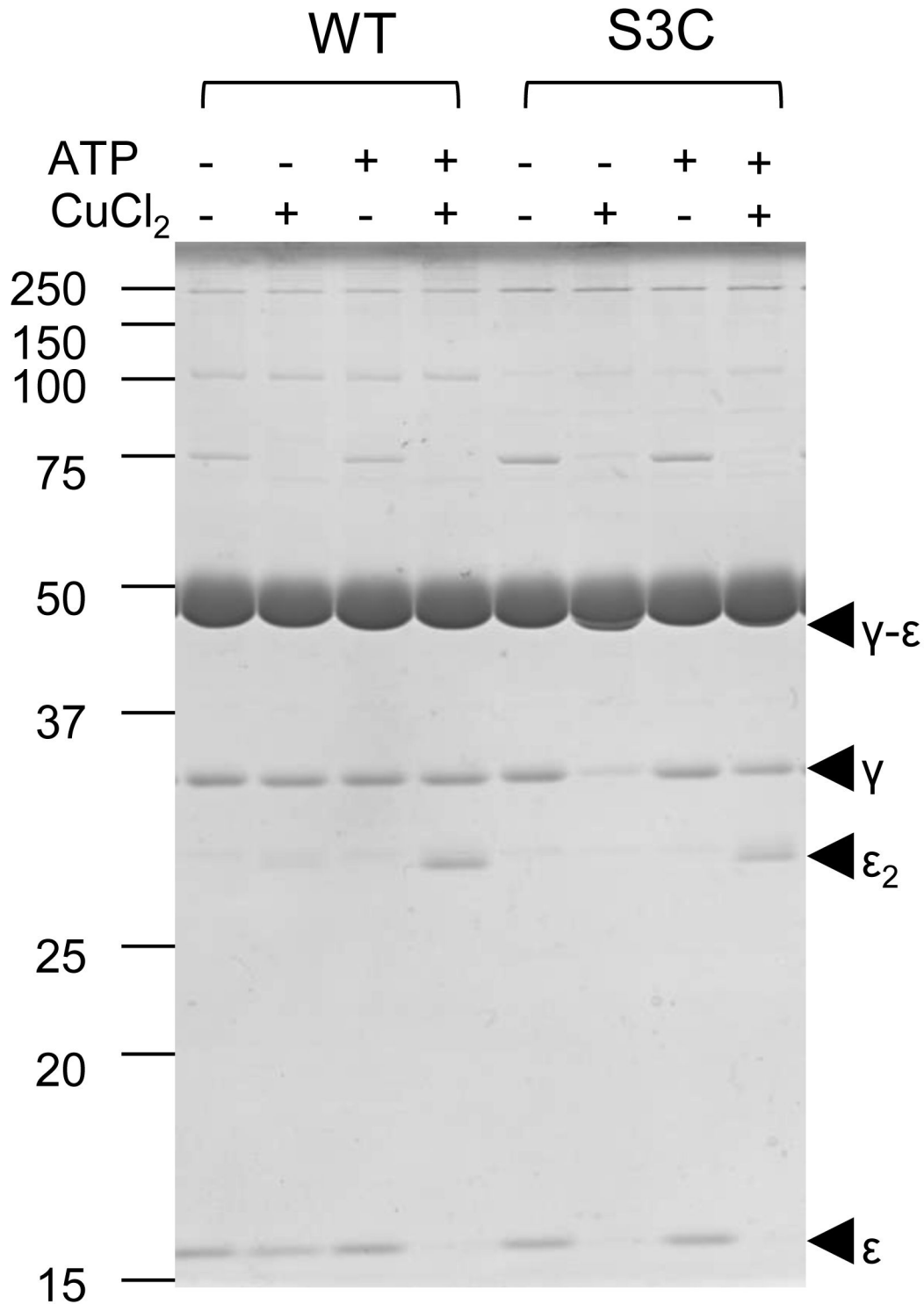


Figure 4. Non-reducing SDS-PAGE analysis of mutant $\alpha_3\beta_3\gamma^{\text{S3C}\epsilon^{133\text{C}}}$. The $\alpha_3\beta_3\gamma^{\text{WT}\epsilon^{133\text{C}}}$ (WT) or $\alpha_3\beta_3\gamma^{\text{S3C}\epsilon^{133\text{C}}}$ (S3C) were incubated for 1 h at 25°C with combinations of 2 mM ATP and 50 μM CuCl₂ as indicated at the top of the figure. After the incubation, the samples were subjected to non-reducing SDS-PAGE (12% acrylamide). Bands derived from γ and ϵ subunits are marked by arrowheads.

doi: 10.1371/journal.pone.0073888.g004

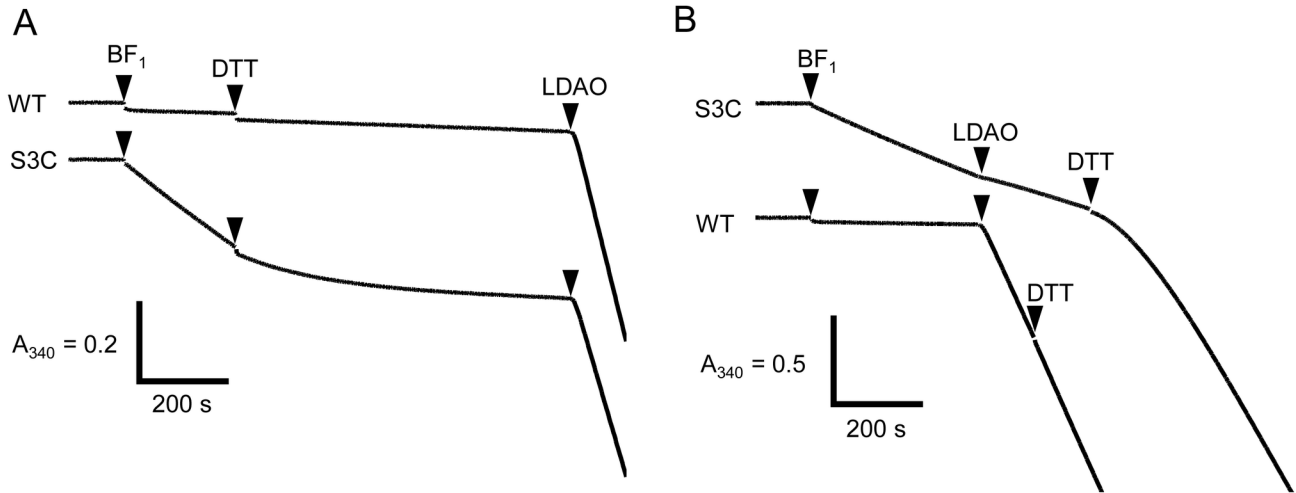


Figure 5. Kinetics of ATP hydrolysis by mutant $\alpha_3\beta_3\gamma^{S3C}\epsilon^{133C}$. ATPase activities of $\alpha_3\beta_3\gamma^{S3C}\epsilon^{133C}$ (S3C), and $\alpha_3\beta_3\gamma^{WT}\epsilon^{133C}$ (WT) at 2 mM ATP were determined. The $\alpha_3\beta_3\gamma\epsilon$ complex of was added to 3 nM at the times indicated by the first arrowheads. (A) DTT (50 mM) and LDAO (0.1%) were added at the times indicated by the second and third arrowheads, respectively. (B) The order of addition of DTT and LDAO was reversed.

doi: 10.1371/journal.pone.0073888.g004

because the relief from MgADP inhibition by the ϵ subunit is more prominent.

Counteraction of MgADP inhibition and ϵ subunit

As discussed above, the ϵ subunit suppressed MgADP inhibition. In the absence of LDAO, the mutant $\alpha_3\beta_3\gamma^{S3C}\epsilon^{133C}$ complex of BF₁ with an extended-state fixed ϵ subunit showed considerably higher ATPase activity than the WT, even at 2 mM ATP. LDAO did not activate the ATPase activity (Figure 5B). Thus, even before the addition of LDAO, the extended-state fixed $\alpha_3\beta_3\gamma^{S3C}\epsilon^{133C}$ complex of BF₁ might be less inhibited by MgADP inhibition. This conclusion is further strengthened by the results when the WT BF₁ was preincubated with MgADP (Figure 3). In the absence of the ϵ subunit, preincubation with MgADP suppressed the ATPase activity of $\alpha_3\beta_3\gamma$ proportionally at a $\alpha_3\beta_3\gamma$: MgADP ratio of 1:2, suggesting that binding of MgADP is strong and binding of one or two MgADP is enough to induce MgADP inhibition of $\alpha_3\beta_3\gamma$ complex. In contrast, greater than 60% of the activity was retained in the presence of 1:2 MgADP and the ϵ subunit, indicating that binding of MgADP to $\alpha_3\beta_3\gamma\epsilon$ was highly suppressed by the ϵ subunit. This agrees well with our previous observation that the ϵ subunit of TF₁ significantly suppresses the binding of MgADP [33]. LDAO did not activate the extended-fixed $\alpha_3\beta_3\gamma^{S3C}\epsilon^{133C}$ complex of BF₁ (Figure 5B), indicating that the extended-state ϵ subunit reduced MgADP inhibition. Considering all of these results, we conclude that ϵ inhibition is not due to the stabilization of MgADP inhibition [28,29,31], but due to an essentially different and counteracting mechanism. We believe, therefore, that these properties must be common among various F₁-ATPases, despite the differences in the mechanisms of ϵ inhibition. It should be noted, however, the ϵ subunit did not protect mutant $\alpha_3\beta_3\gamma^{S3C}\epsilon^{133C}$ complex from MgADP inhibition by the

preincubation with ADP (Figure S1). These apparent contradictory results may be due to the different catalytic site affinity for nucleotides between WT and the mutant (γ^{S3C}) $\alpha_3\beta_3\gamma$ complexes, and/or different mode of the action of MgADP during preincubation and ATPase turnover etc. Further experiments, for example, measurement of nucleotide binding to the catalytic sites with WT and mutant $\alpha_3\beta_3\gamma$ with and without ϵ subunit will give us a clue to resolve the differences between WT and the mutant in the MgADP preincubation experiment.

Significance of regulation by the ϵ subunit and MgADP inhibition in vivo

The results presented here indicate that the ATPase activity of BF₁ is very low under normal conditions due to strong MgADP inhibition. Because *B. subtilis* lives in an aerobic environment and its ATP synthase is primarily used to synthesize ATP but not to hydrolyze ATP, as is the case for bacteria such as *E. coli* that can grow anaerobically. The ϵ subunit may not act as an inhibitor of the ATPase activity of *B. subtilis* ATP synthase. In contrast, its ability to attenuate MgADP inhibition may be its primary role in the regulatory system. Experiments using *B. subtilis* with mutant FoF₁ to address these questions are underway in our laboratory. Elucidation of the balance and the interplay of these two regulatory systems in different bacteria may be required to understand the regulation of bacterial ATP synthases.

Supporting Information

Figure S1. Effect of preincubation with MgADP on $\alpha_3\beta_3\gamma^{S3C}\epsilon^{133C}$. The $\alpha_3\beta_3\gamma^{S3C}$, DTT-treated $\alpha_3\beta_3\gamma^{S3C}\epsilon^{133C}$ and CuCl₂-treated $\alpha_3\beta_3\gamma^{S3C}\epsilon^{133C}$ (5 μ M) were subjected to the same experiment as

shown in Figure 3. Closed circles, open circles and open squares represent α₃β₃γ^{S3C}, DTT-treated α₃β₃γ^{S3Cε^{133C}} and CuCl₂-treated α₃β₃γ^{S3Cε^{133C}}, respectively. Error bars represent standard errors. (TIF)

Figure S2. Enlargement of the part of Figure 4.

The part of Figure 4 is enlarged to visualize γ-ε crosslinked band clearer. Only the region around α, β and γ-ε from α₃β₃γ^{S3Cε^{133C}} (S3C) treated with or without CuCl₂ in the absence of ATP is shown. (TIF)

References

1. Boyer PD (1997) The ATP synthase: a splendid molecular machine. *Annu Rev Biochem* 66: 717–749. doi:10.1146/annurev.biochem.66.1.717. PubMed: 9242922.
2. Kinoshita K Jr, Yasuda R, Noji H (2000) F₁-ATPase: a highly efficient rotary ATP machine. *Essays Biochem* 35: 3–18. PubMed: 12471886.
3. Yoshida M, Muneyuki E, Hisabori T (2001) ATP synthase: a marvellous rotary engine of the cell. *Nat Rev Mol Cell Biol* 2: 669–677. doi: 10.1038/35088558. PubMed: 11533724.
4. Senior AE, Nadanaciva S, Weber J (2002) The molecular mechanism of ATP synthesis by F₁F_o-ATP synthase. *Biochim Biophys Acta* 1553: 188–211. doi:10.1016/S0005-2728(02)00185-8. PubMed: 11997128.
5. Noji H, Yasuda R, Yoshida M, Kinoshita K Jr (1997) Direct observation of the rotation of F₁-ATPase. *Nature* 386: 299–302. doi: 10.1038/386299a0. PubMed: 9069291.
6. Yasuda R, Noji H, Kinoshita K Jr, Yoshida M (1998) F₁-ATPase is a highly efficient molecular motor that rotates with discrete 120 degree steps. *Cell* 93: 1117–1124. doi:10.1016/S0092-8674(00)81456-7. PubMed: 9657145.
7. Smith JB, Sternweis PC, Heppel LA (1975) Partial purification of active δ and ε subunits of the membrane ATPase from *Escherichia coli*. *J Supramol Struct* 3: 248–255. doi:10.1002/jss.400030307. PubMed: 127087.
8. Laget PP, Smith JB (1979) Inhibitory properties of endogenous subunit ε in the *Escherichia coli* F₁ ATPase. *Arch Biochem Biophys* 197: 83–89. doi:10.1016/0003-9861(79)90222-4. PubMed: 161698.
9. Ort DR, Oxborough K (1992) In situ regulation of chloroplast coupling factor activity. *Annu Rev Plant Physiol Plant Mol Biol* 43: 269–291. doi: 10.1146/annurev.pp.43.060192.001413.
10. Kato Y, Matsui T, Tanaka N, Muneyuki E, Hisabori T et al. (1997) Thermophilic F₁-ATPase is activated without dissociation of an endogenous inhibitor, ε subunit. *J Biol Chem* 272: 24906–24912. doi: 10.1074/jbc.272.40.24906. PubMed: 9312092.
11. Rodgers AJW, Wilce MCJ (2000) Structure of the γ-ε complex of ATP synthase. *Nat Struct Biol* 7: 1051–1054. doi:10.1038/80975. PubMed: 11062562.
12. Tsunoda SP, Rodgers AJW, Aggeler R, Wilce MCJ, Yoshida M et al. (2001) Large conformational changes of the ε subunit in the bacterial F₁F_o ATP synthase provide a ratchet action to regulate this rotary motor enzyme. *Proc Natl Acad Sci U S A* 98: 6560–6564. doi:10.1073/pnas.111128098. PubMed: 11381110.
13. Suzuki T, Murakami T, Iino R, Suzuki J, Ono S et al. (2003) FoF₁-ATPase/synthase is geared to the synthesis mode by conformational rearrangement of ε subunit in response to proton motive force and ADP/ATP balance. *J Biol Chem* 278: 46840–46846. doi:10.1074/jbc.M307165200. PubMed: 12881515.
14. Iino R, Murakami T, Izuka S, Kato-Yamada Y, Suzuki T et al. (2005) Real time monitoring of conformational dynamics of the ε subunit in F₁-ATPase. *J Biol Chem* 280: 40130–40134. doi:10.1074/jbc.M506160200. PubMed: 16203732.
15. Feniouk BA, Kato-Yamada Y, Yoshida M, Suzuki T (2010) Conformational transitions of subunit ε in ATP synthase from the thermophilic *Bacillus PS3*. *Biophys J* 98: 434–442. doi:10.1016/j.bpj.2009.12.2357. PubMed: 20141757.
16. Cingolani G, Duncan TM (2011) Structure of the ATP synthase catalytic complex (F₁) from *Escherichia coli* in an autoinhibited conformation. *Nat Struct Mol Biol* 18: 701–707. doi:10.1038/nsmb.2058. PubMed: 21602818.

Acknowledgements

We thank Professor F. Kawamura at Rikkyo University for providing us with *B. subtilis* genomic DNA and members of Y. Kato-Yamada’s laboratory for their help and critical discussions.

Author Contributions

Conceived and designed the experiments: YKY. Performed the experiments: JM YK YN NM AC TO TH YKY. Analyzed the data: JM YK YKY. Wrote the manuscript: JM YKY.

17. Kato S, Yoshida M, Kato-Yamada Y (2007) Role of the ε subunit of the thermophilic F₁-ATPase as a sensor for ATP. *J Biol Chem* 282: 37618–37623. doi:10.1074/jbc.M707509200. PubMed: 17933866.
18. Kadoya F, Kato S, Watanabe K, Kato-Yamada Y (2011) ATP binding to the ε subunit of thermophilic ATP synthase is crucial for efficient coupling of ATPase and H⁺ pump activities. *Biochem J* 437: 135–140. doi:10.1042/BJ20110443. PubMed: 21510843.
19. Vasilyeva EA, Minkov IB, Fitin AF, Vinogradov AD (1982) Kinetic mechanism of mitochondrial adenosine triphosphatase. ADP-specific inhibition as revealed by the steady-state kinetics. *Biochem J* 202: 9–14. PubMed: 6211173.
20. Vasilyeva EA, Minkov IB, Fitin AF, Vinogradov AD (1982) Kinetic mechanism of mitochondrial adenosine triphosphatase. Inhibition by azide and activation by sulphite. *Biochem J* 202: 15–23. PubMed: 6211171.
21. Zhou J-M, Xue ZX, Du ZY, Melese T, Boyer PD (1988) Relationship of tightly bound ADP and ATP to control and catalysis by chloroplast ATP synthase. *Biochemistry* 27: 5129–5135. doi:10.1021/bi00414a027. PubMed: 2901855.
22. Milgrom YM, Ehler LL, Boyer PD (1991) The characteristics and effect on catalysis of nucleotide binding to noncatalytic sites of chloroplast F₁-ATPase. *J Biol Chem* 266: 11551–11558. PubMed: 1828802.
23. Milgrom YM, Cross RL (1993) Nucleotide binding sites on beef heart mitochondrial F₁-ATPase. Cooperative interactions between sites and specificity of noncatalytic sites. *J Biol Chem* 268: 23179–23185. PubMed: 8226836.
24. Hyndman DJ, Milgrom YM, Bramhall EA, Cross RL (1994) Nucleotide-binding sites on *Escherichia coli* F₁-ATPase. Specificity of noncatalytic sites and inhibition at a catalytic sites by MgADP. *J Biol Chem* 269: 28871–28877. PubMed: 7961847.
25. Jault J-M, Matsui T, Jault FM, Kaibara C, Muneyuki E et al. (1995) The α₃β₃γ complex of the F₁-ATPase from thermophilic *Bacillus*. PS 3 containing the αD261N substitution fails to dissociate inhibitory MgADP from a catalytic site when ATP binds to noncatalytic sites. *Biochemistry* 34: 16412–16418.
26. Matsui T, Muneyuki E, Honda M, Allison WS, Dou C et al. (1997) Catalytic activity of the α₃β₃γ complex of F₁-ATPase without noncatalytic nucleotide binding site. *J Biol Chem* 272: 8215–8221. doi: 10.1074/jbc.272.13.8215. PubMed: 9079639.
27. Hirono-Hara Y, Noji H, Nishiura M, Muneyuki E, Hara KY et al. (2001) Pause and rotation of F₁-ATPase during catalysis. *Proc Natl Acad Sci U S A* 98: 13649–13654. doi:10.1073/pnas.241365698. PubMed: 11707579.
28. Konno H, Murakami-Fuse T, Fujii F, Koyama F, Ueoka-Nakanishi H et al. (2006) The regulator of the F₁ motor: inhibition of rotation of cyanobacterial F₁-ATPase by the ε subunit. *EMBO J* 25: 4596–4604. doi:10.1038/sj.emboj.7601348. PubMed: 16977308.
29. Tsumuraya M, Furuike S, Adachi K, Kinoshita K Jr, Yoshida M (2009) Effect of ε subunit on the rotation of thermophilic *Bacillus* F₁-ATPase. *FEBS Lett* 583: 1121–1126. doi:10.1016/j.febslet.2009.02.038. PubMed: 19265694.
30. Haruyama T, Hirono-Hara Y, Kato-Yamada Y (2010) Inhibition of thermophilic F₁-ATPase by the ε subunit takes different path from the ADP-Mg inhibition. *Biophysics* 6: 59–65. doi:10.2142/biophysics.6.59.
31. Feniouk BA, Suzuki T, Yoshida M (2007) Regulatory interplay between proton motive force, ADP, phosphate, and subunit ε in bacterial ATP synthase. *J Biol Chem* 282: 764–772. PubMed: 17092944.

32. Jault J-M, Dou C, Grodsky NB, Matsui T, Yoshida M et al. (1996) The α3β₃γ subcomplex of the F₁-ATPase from the thermophilic *Bacillus*. PS 3 with the BT165S substitution does not entrap inhibitory MgADP in a catalytic site during turnover. *J. Biol. Chem.* 271: 28818-28824.
33. Yasuno T, Muneyuki E, Yoshida M, Kato-Yamada Y (2009) Modulation of nucleotide binding to the catalytic sites of thermophilic F₁-ATPase by the ε subunit: implication for the role of the ε subunit in ATP synthesis. *Biochem Biophys Res Commun* 390: 230–234. doi:10.1016/j.bbrc.2009.09.092. PubMed: 19785990.
34. Sekiya M, Hosokawa H, Nakanishi-Matsui M, Al-Shawi MK, Nakamoto RK et al. (2010) Single molecule behavior of inhibited and active states of *Escherichia coli* ATP synthase F₁ rotation. *J Biol Chem* 285: 42058-42067. doi:10.1074/jbc.M110.176701. PubMed: 20974856.
35. Konno H, Isu A, Kim Y, Murakami-Fuse T, Sugano Y et al. (2011) Characterization of the relationship between ADP- and ε-induced inhibition in cyanobacterial F₁-ATPase. *J Biol Chem* 286: 13423-13429. doi:10.1074/jbc.M110.155986. PubMed: 21345803.
36. Hicks DB, Krulwich TA (1987) Purification and characterization of the F₁ ATPase from *Bacillus subtilis* and its uncoupler-resistant mutant derivatives. *J Bacteriol* 169: 4743–4749. PubMed: 2888751.
37. Hicks DB, Cohen DM, Krulwich TA (1994) Reconstitution of energy-linked activities of the solubilized F₁F_o ATP synthase from *Bacillus subtilis*. *J Bacteriol* 176: 4192–4195. PubMed: 8021203.
38. Santana M, Ionescu MS, Vertes A, Longin R, Kunst F et al. (1994) *Bacillus subtilis* FoF₁ ATPase: DNA sequence of the atp operon and characterization of atp mutants. *J Bacteriol* 176: 6802–6811. PubMed: 7961438.
39. Matsui T, Yoshida M (1995) Expression of the wild-type and the Cys-/Trp-less α₃β₃γ complex of thermophilic F₁-ATPase in *Escherichia coli*. *Biochim Biophys Acta* 1231: 139–146. doi:10.1016/0005-2728(95)00070-Y. PubMed: 7662694.
40. Higuchi R, Krummel B, Saiki RK (1988) A general method of in vitro preparation and specific mutagenesis of DNA fragments: study of protein and DNA interactions. *Nucleic Acids Res* 16: 7351–7367. doi:10.1093/nar/16.15.7351. PubMed: 3045756.
41. Ho SN, Hunt HD, Horton RM, Pullen JK, Pease LR (1989) Site-directed mutagenesis by overlap extension using the polymerase chain reaction. *Gene (Amst.)*77: 51–59.
42. Kato-Yamada Y, Yoshida M (2003) Isolated ε subunit of thermophilic F₁-ATPase binds ATP. *J Biol Chem* 278: 36013–36016. doi:10.1074/jbc.M306140200. PubMed: 12837747.
43. Hisabori T, Muneyuki E, Odaka M, Yokoyama K, Mochizuki K et al. (1992) Single site hydrolysis of 2', 3'-O-(2,4,6-trinitrophenyl)-ATP by the F₁-ATPase from thermophilic bacterium. PS 3 is accelerated by the chase-addition of excess ATP. *J. Biol. Chem.* 267: 4551–4556
44. Stiggall DL, Galante YM, Hatefi Y (1979) Preparation and properties of complex V. *Methods Enzymol* 55: 308–315. doi:10.1016/0076-6879(79)55036-8. PubMed: 156835.
45. Bradford MM (1976) A rapid and sensitive method for the quantitation of microgram quantities of protein utilizing the principle of protein-dye binding. *Anal Biochem* 72: 248–254. doi:10.1016/0003-2697(76)90527-3. PubMed: 942051.
46. Laemmli UK. (1970) Cleavage of structural proteins during the assembly of the head of bacteriophage T4. *Nature* 227: 680-685. doi:10.1038/227680a0. PubMed: 5432063.
47. Kato Y, Sasayama T, Muneyuki E, Yoshida M (1995) Analysis of time-dependent change of *Escherichia coli* F₁-ATPase activity and its relationship with apparent negative Cooperativity. *Biochim Biophys Acta* 1231: 275–281. doi:10.1016/0005-2728(95)00087-Y. PubMed: 7578215.
48. Bald D, Muneyuki E, Amano T, Kruij J, Hisabori T et al. (1999) The noncatalytic site-deficient α₃β₃γ subcomplex and FoF₁-ATP synthase can continuously catalyze ATP hydrolysis when Pi is present. *Eur J Biochem* 262: 563–568. doi:10.1046/j.1432-1327.1999.00410.x. PubMed: 10336643.
49. Bald D, Amano T, Muneyuki E, Pitard B, Rigaud JL et al. (1998) ATP synthesis by FoF₁-ATP synthase independent of noncatalytic nucleotide binding sites and insensitive to azide inhibition. *J Biol Chem* 273: 865–870. doi:10.1074/jbc.273.2.865. PubMed: 9422743.